

Modeling of NO_x Formation in Natural Gas Fueled Diesel Combustion

Y.Yosihara, H.Wang* and M.Frenklach*

*Department of Mechanical Engineering
Ritsumeikan University
1916 Nojicho, Kusatsu, Shiga, 525-77
Japan*

** The Pennsylvania State University*

ABSTRACT

A model for predicting the formation and destruction of nitrogen oxides and their emissions from a natural gas fueled diesel engine has been developed by taking chemical kinetics into account. The stochastic approach was used to model fluid dynamic behavior in the combustion chamber by assuming the turbulent mixing is a random mixing processes among fine fluid particles.

The calculations were made under the same conditions as the experiments. The mixing rate or collision frequency was chosen to fit the pressure and heat release rate with those of the experiments. It is shown that the model reproduces the pressure history of the experiments well and the predicted NO concentration at exhaust coincides with that of the experiments within a factor of 1.5. The results also show that most NO is formed locally at temperatures higher than 2500 K under a range of fuel-air equivalence ratios, $0.8 < \phi < 1$ and that the NO, once formed, is hardly destroyed through combustion.

INTRODUCTION

Reducing nitrogen oxides emitted from a diesel engines requires urgent attention to prevent further worldwide air pollution. At present, however, reduction methods that do not sacrifice heat efficiency are still unclear. To obtain a solution, there is a need to clarify the origin of the nitric oxide generation and its destruction during diesel combustion. Almost all nitric oxide in the exhaust can be formed locally at the region having the highest temperature and fuel lean equivalence ratio in the combustion chamber. The generation from such regions may strongly depend not only on turbulent mixing but also on slow chemical reactions such as ignition processes. Furthermore, as is well known, NO formation itself, under the high temperature, is controlled by a slow chemical mechanism. Therefore,

it is important for modeling the NO formation during diesel combustion, to take both the turbulent mixing and the detailed chemical kinetics into account. However, the multidimensional model for diesel combustion (1-3) does not seem practical at present, because long computation time will be required if detailed chemical mechanism is taken into account. On the other hand, the stochastic model for diesel combustion (4) developed by Ikegami et al., seems suitable for this problem. This model relies on the concept that combustion evolves by random collision and coalescence of individual fluid particles. This allows the description of heterogeneity of the fuel concentration without relying upon the concept of space that is indispensable to the deterministic approach. Therefore, it is easy for this model to introduce detailed chemical kinetics with a reasonable increase of computation time. As for ignition processes, unfortunately, the original model does not take the detailed chemical kinetics into account and, with regard to NO formation, considers only the Zeldvich mechanism. In a practical system such as diesel combustion, it is not known whether the destruction of NO is controlled by the Zeldvich mechanism only or not.

In the present study, the stochastic model was extended, taking into consideration a detailed chemical mechanism for both processes of the initiation and the NO formation, to test the origin of NO emission. We carried out a computer simulation of NO formation for natural gas fueled, high-speed direct-injection diesel engines under the condition of an actual experiment (5).

STOCHASTIC MODEL

A stochastic approach for diesel combustion (4) was employed in the present study. In this model the heterogeneity and its devolution are described using the Curl collision-redispersion model (6) and thermodynamic states of fluid are expressed by probability density functions. The turbulent mixing is

described by random collision and coalescence of individual fluid particles. These collision and coalescence occurred at the intervals related to turbulent intensity between two individual fluid particles chosen at random. The composition of each fluid cell is homogeneous and changes continuously with time under the control of chemical kinetics.

Basic equations

The state of a fluid is described by assigning the pressure p , the specific enthalpy h , and the mole number of species y_j ($j=1,n$). According with the stochastic model mentioned above, since pressure is uniform at every moment, the probability density function is defined $f=f(\mathbf{x},t)$, where $\mathbf{x}=(h, y_1, \dots, y_j, \dots, y_n)$ denotes state vector and the master equation is given by

$$\frac{\partial f}{\partial t} + \frac{\partial h f}{\partial h} + \sum_j \frac{\partial y_j f}{\partial y_j} = \omega \phi(\mathbf{x}, t) \quad (1)$$

$$\phi(\mathbf{x}, t) = \iint 2f(\mathbf{x}^{(1)}, t) f(\mathbf{x}^{(2)}, t) \delta \left\{ \frac{h^{(1)} + h^{(2)}}{2} - h \right\} \prod_j \delta \left\{ \frac{y_j^{(1)} + y_j^{(2)}}{2} - y_j \right\} d\mathbf{x}^{(1)} d\mathbf{x}^{(2)} - 2f(\mathbf{x}, t) \quad (2)$$

where $\phi(\mathbf{x}, t)$ denotes the extended Curl collision function, ω the collision frequency or the probability of collision for a fluid particle during a unit time, and δ the Dirac's delta function. Eq.(1) shows that the change of the probability density function with time is given from the changes of state vector due to collision.

To describe the probability density function, a large amount of fluid particle having the same mass is taken into account in the calculation. From the first law of thermodynamics and equation of state for ideal gas, pressure change is given as the function of the cylinder volume V_c and composition of each particle as follows.

$$\frac{dp}{dt} = \frac{m \sum_i T_i \frac{dR_i}{dt} - m \sum_i R_i \frac{\sum_j h_j y_{ij} + \dot{q}_i}{\sum_j c_{pj} y_{ij}} - p \frac{dV_c}{dt}}{V_c - m \sum_i \frac{R_i V_i}{\sum_j c_{pj} y_{ij}}} \quad (3)$$

Where m is the mass of particle, R_i the gas constant for i -th particle, h_i the enthalpy of i -th particle, y_{ij} the mole number of j -th species in i -th particle, c_{pj} the specific heat at constant pressure for species j , and \dot{q}_i the heat loss for i -th particle. Since dy_{ij}/dt can be determine by kinetics, we can get dp/dt from Eq.(3). dT_i/dt is given from the first law of thermodynamics as the function of dp/dt .

$$\frac{dT_i}{dt} = \frac{V_i \frac{dp}{dt} - \sum_j h_j \frac{dy_{ij}}{dt} - \dot{q}_i}{\sum_j c_{pj} y_{ij}} \quad (4)$$

In summary, the diesel combustion model based on the stochastic approach results in solving Eqs.(1)-(4) simultaneously.

Reactions

At the present stage of this study, the diesel engine fueled natural gas was studied in place of the engine fueled commercial gas oil since the detailed chemical mechanism of natural gas has been developed and NO formation in natural gas fueled diesel engine is not far from that in normal diesel engines. Although the primary concern of the present study is the NO formation, accurate prediction for the initiation or ignition process is critical for quantitative modeling of NO formation. These considerations underlie our interest in maintaining this chemical model as realistic as possible, while keeping its size to the minimum possible. The initial, "full" reaction mechanism for methane combustion was taken from Ref. (7). It was reduced in size at the conditions typical of diesel combustion to a 21-species mechanism, listed as reaction 1-74 in Table 1. This mechanism includes chemistry for C_2H_6 but excludes that for C_3H_8 . Usually, natural gas contains a small amount of propane and butane in addition to methane and ethane. Therefore, the set of reactions 1-74 was augmented with dissociation of propane, reactions 75 (Table 1). The butane in the fuel was incorporated into propane, in order to restrict the size of the reaction set.

For NO formation, the Skeletal mechanism (8) was used in the present study. This mechanism includes the Zeldvich mechanism, prompt NO mechanism and destruction of NO by NH_2 .

Computational Procedure

We present computer simulations of NO formation for the combustion of natural gas in a glow-assisted direct-injection diesel engine. The computations were carried out under the conditions of an actual experiment(5): engine speed 1800 rpm, single cylinder, water cooled, naturally-aspirated, four cycle, swirl ratio 2.7, compression ratio 16, fuel-air equivalence ratio 0.65. When the equivalence ratio was 0.65, a total 197 cells of equal mass, 190 of air and 7 of fuel, were considered. The collision frequency, which depends on the total number of particles considered in the calculation, was obtained by fitting the rate of heat release. In the present study, collision occurred with a constant frequency, $2.5 \mu s$ during the fuel injection and $10 \mu s$ after injection. Heat losses were estimated with Annand and Ma's empirical formula (9).

Table 1 Mechanism of methane oxidation and NO formation

No. Reaction ^a	k = AT ⁿ exp(-E/RT)		
	A (cm, mol, s)	n	E (kJ mol ⁻¹)
1 H + O2 = OH + O	5.33D+16	-.750	72.000
2 O + H2 = OH + H	3.87D+04	2.700	26.200
3 OH + H2 = H2O + H	2.16D+08	1.510	14.350
4 OH + OH = O + H2O	2.10D+08	1.400	-1.660
5 H + O2 + M = HO2 + M	7.00D+17	-.800	.000
ETBE ^b H2=0.0 CO2=0.0 O2=0.0 N2=0.0 H2O=0.0 CO=0.0			
6 H + O2 + H2 = HO2 + H2	2.80D+18	-.860	.000
7 H + O2 + O2 = HO2 + O2	3.00D+20	-1.720	.000
8 H + O2 + N2 = HO2 + N2	3.75D+20	-1.720	.000
9 H + O2 + CO = HO2 + CO	2.10D+18	-.860	.000
10 H + O2 + CO2 = HO2 + CO2	4.10D+18	-.860	.000
11 H + O2 + H2O = HO2 + H2O	9.40D+18	-.760	.000
12 HO2 + H = OH + OH	1.50D+14	.000	4.200
13 HO2 + H = H2 + O2	2.50D+13	.000	2.900
14 HO2 + O = O2 + OH	2.00D+13	.000	.000
15 HO2 + OH = H2O + O2	6.02D+13	.000	.000
16 HO2 + HO2 = H2O2 + O2	1.06D+11	.000	-7.100
17 H2O2 + M = OH + OH + M	1.00D+17	.000	190.000
ETBE ^b H2=2.9 CO2=4.3 O2=1.2 N2=1.2 H2O=18.5 CO=2.1			
18 H2O2 + OH = H2O + HO2	7.00D+12	.000	6.000
19 HOCO (+M) = H + CO2 (+M) ^c	1.74D+12	.310	137.825
LOW PRES. LIMIT	6.44D+29	-4.440	149.559
SRI DATA.	0.683	534.32	10777.07
20 HOCO (+M) = CO + OH (+M) ^c	5.89D+12	.530	142.226
LOW PRES. LIMIT	6.16D+26	-3.310	150.459
SRI DATA.	0.467	454.32	8483.82
21 CO + OH = CO2 + H	1.22D+07	1.350	-2.640
22 CO + HO2 = CO2 + OH	1.50D+14	.000	98.700
23 CO + O + M = CO2 + M	3.01D+14	.000	12.600
ETBE ^b H2=0.0 CO2=7.0 O2=12.0 N2=2.0 H2O=0.0 CO=3.0			
24 CO + O2 = CO2 + O	2.50D+12	.000	200.000
25 CHO + H = H2 + CO	7.23D+13	.000	.000
26 CHO + OH = H2O + CO	1.00D+14	.000	.000
27 CHO + O2 = HO2 + CO	4.20D+12	.000	.000
28 CHO + M = H + CO + M	1.86D+17	-1.000	71.100
ETBE ^b H2 = 1.9 CO2=1.0 O2=1.0 N2=1.0 H2O=8.1 CO=0.0			
29 CH2S + H2 = CH3 + H	7.23D+13	.000	.000
30 CH2S + O2 = CO + OH + H	3.10D+13	.000	.000
31 CH2S + M = CH2 + M	6.00D+12	.000	.000
ETBE ^b H2=2.4 CO2=3.6 O2=1.0 N2=1.0 H2O=15.4 CO=1.8			
32 CH2 + O2 = CO2 + H + H	1.60D+12	.000	4.180
33 CH2 + O2 = CH2O + O	5.00D+13	.000	37.700
34 CH2O + H = CHO + H2	1.26D+08	1.620	9.100
35 CH2O + O = CHO + OH	3.50D+13	.000	14.700
36 CH2O + OH = CHO + H2O	7.23D+05	2.460	-4.060
37 CH2O + O2 = CHO + HO2	1.00D+14	.000	167.000
38 CH2O + HO2 = CHO + H2O2	1.00D+12	.000	33.500
39 CH2O + CH3 = CHO + CH4	8.91D-13	7.400	-4.000
40 CH2O + M = CHO + H + M	5.00D+16	.000	320.000
ETBE ^b H2=2.9 CO2=4.3 O2=1.2 N2=1.2 H2O=18.5 CO=2.1			
41 CH3 + H = CH2 + H2	1.80D+14	.000	63.200
42 CH3 + O = CH2O + H	8.43D+13	.000	.000
43 CH3 + OH = CH2O + H2	8.00D+12	.000	.000
44 CH3 + OH = CH2 + H2O	1.13D+06	2.130	10.200
45 CH3 + O2 = CH3O + O	4.30D+13	.000	128.900
46 CH3 + O2 = CH2O + OH	5.20D+13	.000	146.000
47 CH3 + HO2 = CH3O + OH	2.28D+13	.000	.000
48 CH3 + CHO = CH4 + CO	3.20D+11	.500	.000
49 CH3 + CH3 = C2H5 + H	4.90D+12	.000	49.100
50 CH3 + CH2 = C2H4 + H	5.00D+13	.000	.000
51 CH4 (+M) = CH3 + H (+M) ^c	7.05D+16	-.558	438.909
LOW PRES. LIMIT	1.19D+35	-4.911	447.562
SRI DATA.	0.555	405.62	4580.86
52 CH4 + H = CH3 + H2	7.80D+06	2.110	32.400
53 CH4 + O = CH3 + OH	1.90D+09	1.440	36.300
54 CH4 + O2 = CH3 + HO2	8.00D+13	.000	234.300
55 CH4 + OH = CH3 + H2O	1.50D+06	2.130	10.200
56 CH4 + HO2 = CH3 + H2O2	1.12D+13	.000	103.100
57 CH3O + O2 = CH2O + HO2	4.28D-13	7.600	-14.760

Table 1 (continued)

No. Reaction ^a	k = AT ⁿ exp(-E/RT)		
	A (cm, mol, s)	n	E (kJ mol ⁻¹)
58 CH3O + CO = CO2 + CH3	4.68D+02	3.160	22.500
59 CH3O + M = CH2O + H + M	1.00D+14	.000	105.000
ETBE ^b H2=2.9 CO2=4.3 O2=1.2 N2=1.2 H2O=18.5 CO=2.1			
60 C2H3 + H = C2H2 + H2	3.00D+13	.000	.000
61 C2H3 + O2 = CH2O + CHO	3.98D+12	.000	-1.000
62 C2H4 + H = C2H3 + H2	3.16D+11	.700	33.500
63 C2H4 + O = C2H3 + OH	7.11D+08	1.550	31.340
64 C2H4 + OH = C2H3 + H2O	3.00D+13	.000	12.500
65 C2H4 + CH3 = C2H3 + CH4	3.92D+12	.000	54.500
66 C2H4 + M = C2H3 + H + M	3.80D+17	.000	410.700
ETBE H2=2.9 CO2=4.3 O2=1.2 N2=1.2 H2O=18.5 CO=2.1			
67 C2H5 + O2 = C2H4 + HO2	2.90D+12	.000	20.900
68 C2H5 (+M) = C2H4 + H (+M) ^c	4.97D+10	.730	154.228
LOW PRES. LIMIT	6.24D+39	-6.800	177.800
SRI DATA.	0.667	653.88	8733.74
69 C2H6 (+M) = CH3 + CH3 (+M) ^c	7.10D+25	-2.792	389.670
LOW PRES. LIMIT	2.23D+61	-11.992	414.847
SRI DATA.	0.805	302.71	10730.56
70 C2H6 (+M) = C2H5 + H (+M) ^c	8.85D+20	-1.230	427.777
LOW PRES. LIMIT	1.27D+46	-7.810	450.854
SRI DATA.	0.603	759.32	10869.84
71 C2H6 + H = C2H5 + H2	5.40D+02	3.500	21.800
72 C2H6 + O = C2H5 + OH	1.40D+00	4.300	11.570
73 C2H6 + OH = C2H5 + H2O	2.20D+07	1.900	4.700
74 C2H6 + CH3 = C2H5 + CH4	5.50D-01	4.000	34.700
75 C3H8 = CH3 + C2H5	7.90D+22	-1.790	371.000
76 NH3 + H = NH2 + H2	6.40D+05	2.390	42.470
77 NH3 + O = NH2 + OH	1.10D+06	2.100	21.760
78 NH3 + OH = NH2 + H2O	4.70D+06	1.900	2.090
79 NH2 + H = NH + H2	4.00D+13	.000	15.270
80 NH2 + O = NO + H + H	6.60D+14	-.500	.000
81 NH2 + O = NH + OH	7.00D+12	.000	.000
82 NH2 + OH = NH + H2O	4.00D+06	2.000	4.180
83 NH2 + NO = N2 + H2O	1.30D+16	-1.250	.000
84 NH + H = N + H2	3.20D+13	.000	1.360
85 NH + O = NO + H	7.80D+13	.000	.000
86 NH + OH = NO + H + H	2.00D+13	.000	.000
87 NH + OH = N + H2O	5.00D+11	.500	8.370
88 NH + NO = N2O + H	4.30D+14	-.500	.000
89 N + OH = NO + H	3.80D+13	.000	.000
90 N + O2 = NO + O	6.40D+09	1.000	27.280
91 N + NO = O + N2	3.30D+12	0.300	.000
92 O + N2 + M = N2O + M	1.40D+08	1.430	74.100
93 N2O + H = N2 + OH	1.90D+06	2.420	56.530
94 N2O + O = NO + NO	1.00D+14	0.000	117.990
95 N2O + O = N2 + O2	1.00D+14	0.000	117.990
96 CN + H2 = HCN + H	3.00D+05	2.450	9.360
97 HCN + O = NCO + H	1.40D+04	2.640	20.790
98 HCN + OH = CN + H2O	1.50D+13	0.000	45.610
99 HCN + OH = NH2 + CO	4.40D+02	2.980	39.140
100 CN + O = CO + N	1.80D+13	0.000	.000
101 CN + OH = NCO + H	6.00D+13	0.000	.000
102 CN + O2 = NCO + O	2.60D+14	-0.500	.000
103 NCO + H = NH + CO	5.00D+13	0.000	.000
104 NCO + H2 = NH2 + CO	8.60D+12	0.000	37.660
105 NCO + NO = N2O + CO	1.00D+13	0.000	-1.670
106 CO2 + N = NO + CO	8.60D+11	0.000	9.250
107 CH3 + N = HCN + H + H	7.10D+13	0.000	.000
108 CH2 + NO = NCO + H2	3.50D+12	0.000	-4.600
109 CH + N2 = HCN + N	4.40D+12	0.000	92.050
110 CH + NO = HCN + O	1.00D+14	0.000	.000
111 C + N2 = CN + N	6.30D+13	0.000	192.460
112 C + NO = CN + O	1.90D+13	0.000	.000
113 C + NO = N + CO	2.90D+13	0.000	.000
114 HCCO + NO = HCN + CO2	2.00D+13	0.000	.000

a Reactions with sign "=" were treated as reversible.

b ETBE shows the enhanced third-body efficiencies.

c The pressure dependence of the rate coefficients were treated based on the SRI form.

Calculations were carried out by a step-by-step numerical integration. An implicit manner was used for chemical kinetic calculation. Pressure and temperature of each particle was calculated in an explicit manner. When the mole fraction of OH in a particle exceeds 10^{-5} and that of CH_4 was below 10^{-2} , a state of partial equilibrium was assumed to save computation time. The NO and intermediates, whose formation was controlled by slow kinetics, HCN , CN , NCO , N , NH , NH_2 , N_2O were calculated kinetically at any given moment. To check if the partial equilibrium assumption gives accurate results, several preliminary calculations regarding single particles has been carried out under constant temperature and pressure. Fig. 1, an example of those calculations, shows the concentration of some major species and temperature in an ignition process of natural gas-air mixture obtained by the full kinetic calculation and by the method of present study assuming a state of partial equilibrium after ignition. As for the full kinetic calculation, immediately after OH concentration reaches 10^{-5} in mole fraction, heat is released instantaneously and the state reaches equilibrium. The calculations done under various initial temperature T_0 and fuel-air equivalence ratio ϕ show the same tendency. From these results, therefore, it is noted that the assumption of partial equilibrium used in the present study is likely.

RESULTS AND DISCUSSION

Figure 2 shows a comparison of predicted pressure history and heat release rate with those at the experiment. The Runs 1 and 2 were performed under identical conditions except for different stochastic sequence of fluid particle collisions, originating from different "seed" numbers for the random number generator. These two runs test the "reproducibility" of the stochastic simulations. The difference of pressure and heat release rate obtained in these runs shows that 197 particles are not statistically sufficient to describe heterogeneity. (The number of particle considered in a calculation is restricted by the CPU time. The typical run using a workstation (HP-715/32) took about 12 hours of CPU time.) In the actual engine, however, cycle to cycle variation shows several percents of difference in pressure history. Although, of course, these variations can not be explained by the low number of particles used in this study, the difference in pressure history due to statistical variance nevertheless appears to be at an acceptable level.

Furthermore, the close proximity to the experiment indicates that the parameters used in the calculation seems likely. It should be noted that the predicted heat release rate indicates shorter ignition time lag than that at the experiment. One is an overestimate of the glow assistance, the other is the

constant collision frequency. The collision frequency depends on turbulent characteristics such as turbulent intensity and dissipation rate, should be treated as a function of a time for a precise prediction. In the present study, however, these treatments were not chosen on account of focusing on NO formation rather than precise prediction.

The space averaged NO concentrations in Run1 and Run2 and these mean values are shown in Fig. 3. The NO concentration obtained by the calculation taking into account only the Zeldvich mechanism as the NO formation is also displayed by the curve marked Run3. The collision sequence is the same as that in Run1. The variance of NO concentration between two runs, as mentioned above, comes from the low number of particles used in this study. However, the mean value of those at 60° ATDC., where NO formation freezes, is very close to the experimental

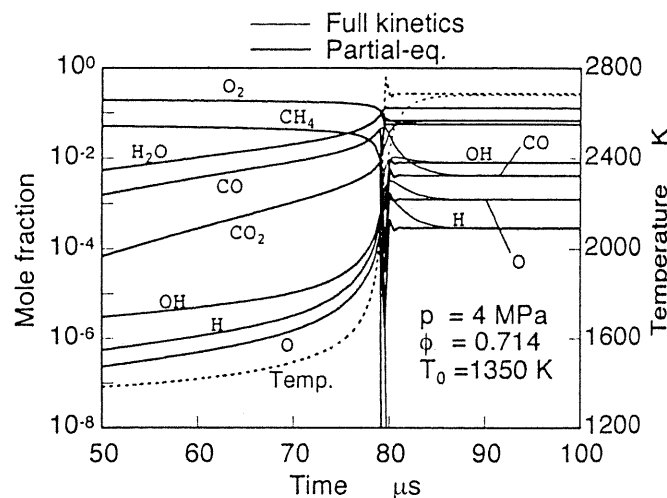


Fig. 1 Concentration of some major species in a ignition process of natural gas-air mixture

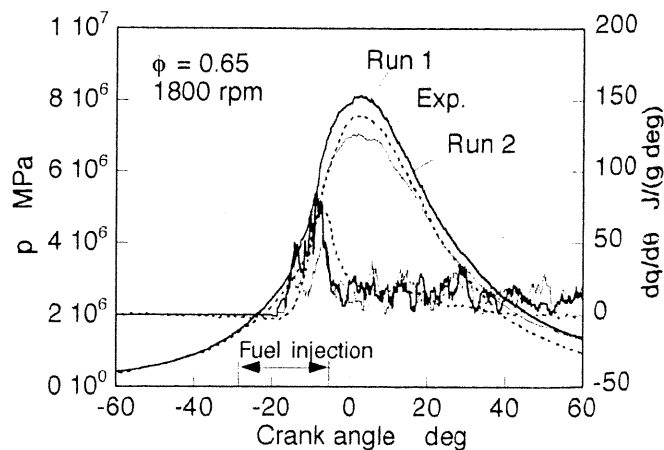


Fig. 2 Pressure history and heat release rate

value of 1020 ppm (5) at exhaust. By comparing Run3 with Run1, it is apparent that the Zeldvich mechanism is not sufficient to predict real NO formation during diesel combustion. The results also suggest that the destruction of NO in a deoxidization circumstance, which is realized by the collision between fuel-lean and fuel-rich particle, is not controlled by only the Zeldvich mechanism

The calculated average concentration of some major species in the case of Run1 is displayed in Fig. 4, versus crank angle. The average temperature and its deviation are shown in Fig. 5. Inspection of these results indicates that most NO is formed around the early stage of the diffusive combustion where the deviation of temperature is high and that NO, once formed, is hardly destroyed through expansion stroke. Fig. 6 shows the correlation between NO and temperature at 1.6° ATDC where NO formation becomes intensive, and Fig. 7 shows that between NO and equivalence ratio. These results indicate that most NO is formed in a small number of particles, having higher temperatures than 2500 K and fuel lean equivalence ratio in the range of $0.8 < \phi < 1$. The above results also suggest that the turbulent mixing process during ignition time lag and explosive combustion strongly depends on NO formation which occurs subsequently during the early stage of the diffusive combustion.

To see the effects of fuel injection timing on NO formation, the calculations have been performed under the same collision sequence as Run 1. It is noted that the results calculated under the same collision sequence are comparable to each other even in the case of having different injection timing. The space averaged NO concentrations and temperatures are displayed in Fig. 8. Early fuel injection elevates the NO level due to the increase of average temperature. In comparison with the experiments, the present model well explain the real tendency of NO increment at early injection, though absolute value does not coincide with that in experiments exactly owing to the low number of particles used in this study mentioned above.

CONCLUSIONS

Stochastic simulations of NO formation were performed for the combustion of natural gas in a glow-assisted direct-injection diesel engine. The simple fluid dynamic method of Curl (6) was employed, which describes turbulent mixing by random collision and coalescence of individual fluid particles. The composition of each fluid particle is homogeneous and changes with time under the control of the chemical kinetics.

It is shown that the predicted NO concentration at exhaust coincides with that of the experiments within a factor of 1.5. The results also show that

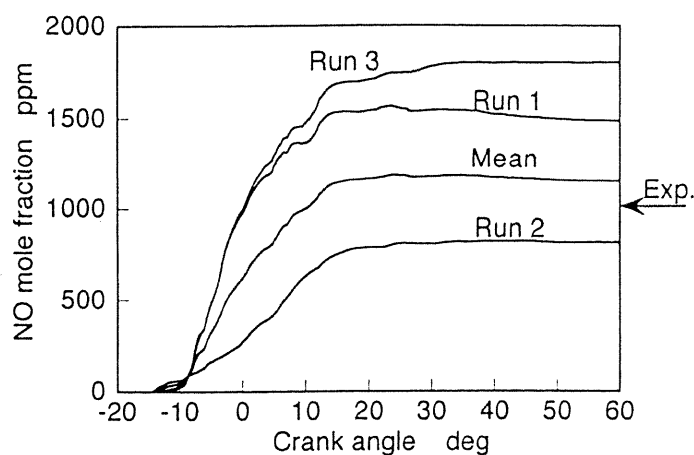


Fig. 3 The space averaged NO concentrations

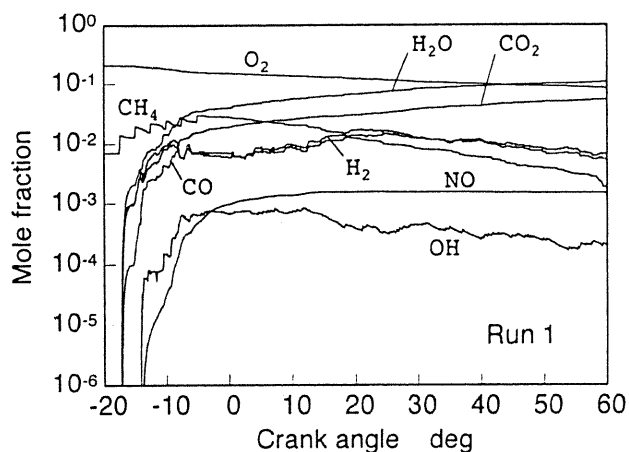


Fig. 4 The calculated average concentration of some major species (Run1)

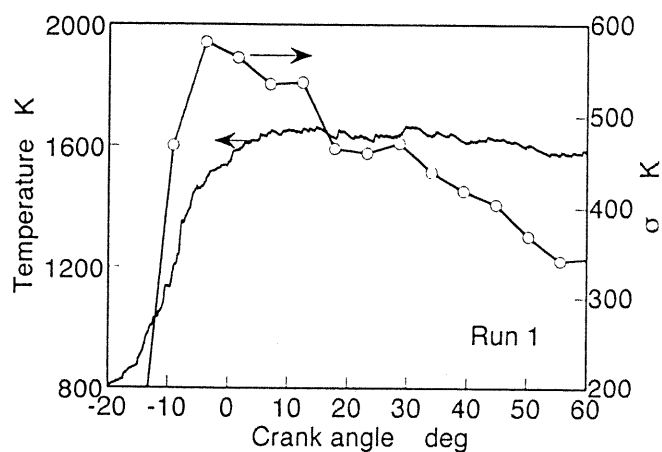


Fig. 5 The average temperature and its deviation (Run1)

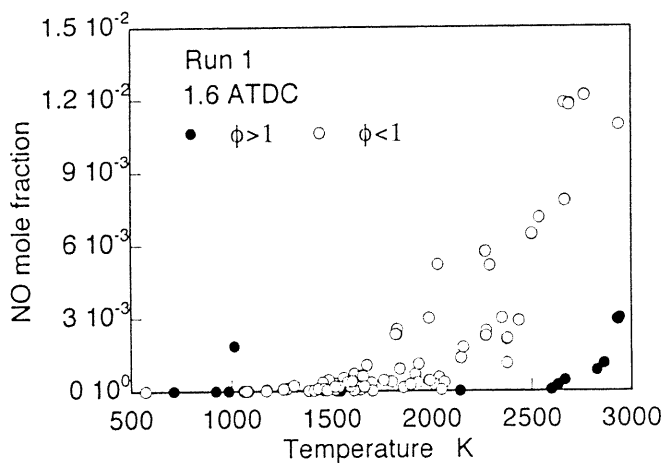


Fig. 6 Correlation between NO and temperature at 1.6° ATDC

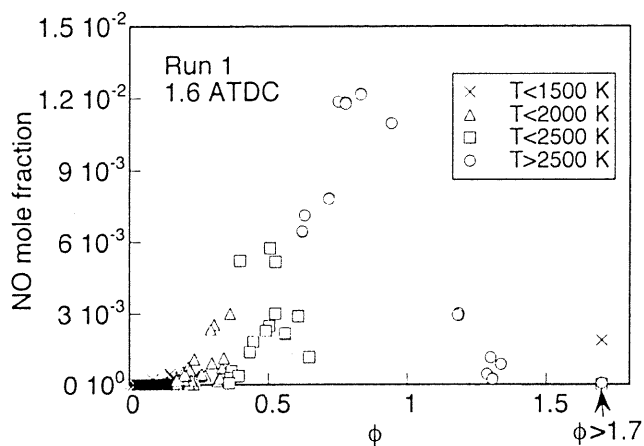


Fig. 7 Correlation between NO and equivalence ratio at 1.6° ATDC

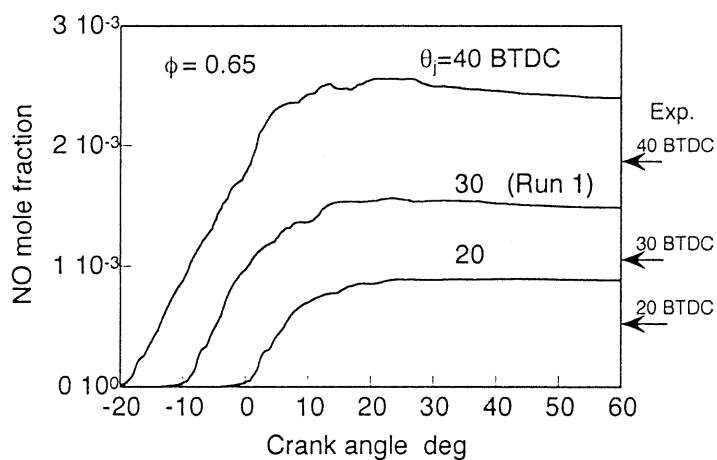


Fig. 8 Space averaged NO concentrations and temperatures at various injection timing

most NO is formed locally at temperatures higher than 2500 K under a range of fuel-air equivalence ratios, $0.8 < \phi < 1$ and that the NO, once formed, is hardly destroyed through combustion. Analysis of NO formation channels suggest that the destruction of NO in a deoxidization circumstance, which is realized by the collision between fuel-lean and fuel-rich particle, is not controlled by only the Zeldovich mechanism.

ACKNOWLEDGMENT

The work at Pennsylvania State University was partially supported by the Gas Research Institute, Contract No. 5092-260-2454. The computations were performed using the facilities of Pennsylvania State University Center for Academic Computing and Ritsumeikan Data Processing Center.

REFERENCES

1. Begleris, P, Gosman, A.D. and Witelaw, J.H., "Measurements and Calculations of the Flow in a Research Diesel Engine" SAE Paper, Paper No. 861563, 1986.
2. Pinchon, Ph., "Three Dimensional Modeling of Combustion in a Prechamber Diesel Engine," SAE Paper, Paper No. 890665, 1989.
3. Ishiguro, J., Kidoguchi, Y. and Ikegami, M., "Three- Dimensional Simulation of the Diesel Combustion Process," JSME Int. Journal, Vol. 31, No. 1, pp. 158-165, 1988.
4. Ikegami, M., Shioji, M. and Koike, M., "A Stochastic Approach to Model the Combustion Process in Direct-Injection Diesel Engines," Twentieth Symp. (Int.) on Comb., pp. 217-224, 1984.
5. Ikegami, M., Shioji, M., Zhu, Q., Hotta, Y. and Endo, H., "A Study of a Direct-Injection High-Compression Engine Fueled with CNG," JSAE, Vol. 24, No. 4, pp. 64-69, 1993 (in Japanese).
6. Curl, R. L., AICHE Journal, "Dispersed Phase Mixing: I. Theory and Effects in Simple Reactors," Vol. 9, No. 2, pp. 175-181, 1963.
7. Frenklach, M., Wang, H. and Rabinowitz, M., "Optimization and Analysis of Large Chemical Kinetic Mechanisms Using the Solution Mapping Method—Combustion of Methane," Prog. Energy Combust. Sci., Vol. 18, pp. 47-73, 1992.
8. Lilleheie, N.I., Byggstoyl, M. and Magnussen, B.F., "Modeling And Chemical Reactions", Nordic Gas Technology Center, pp. 28-30, 1992,
9. Annand, W.J.D. and Ma, T.H., "Instantaneous Heat Transfer Rates to the Cylinder Head Surface of a Small Compression-Ignition Engine," Proc. Instn. Mech. Engrs., Vol. 185, No. 72/71, pp. 976-987, 1970-71.